

## MIT Open Access Articles

*Low contact resistivity of metals on nitrogen-doped cuprous oxide (Cu<sub>2</sub>O) thin-films*

The MIT Faculty has made this article openly available. **Please share** how this access benefits you. Your story matters.

**Citation:** Siah, Sin Cheng et al. "Low Contact Resistivity of Metals on Nitrogen-doped Cuprous Oxide (Cu<sub>2</sub>O) Thin-films." *Journal of Applied Physics* 112.8 (2012): 084508. © 2012 American Institute of Physics

**As Published:** <http://dx.doi.org/10.1063/1.4758305>

**Publisher:** American Institute of Physics (AIP)

**Persistent URL:** <http://hdl.handle.net/1721.1/78017>

**Version:** Final published version: final published article, as it appeared in a journal, conference proceedings, or other formally published context

**Terms of Use:** Article is made available in accordance with the publisher's policy and may be subject to US copyright law. Please refer to the publisher's site for terms of use.



## Low contact resistivity of metals on nitrogen-doped cuprous oxide (Cu<sub>2</sub>O) thin-films

Sin Cheng Siah, Yun Seog Lee, Yaron Segal, and Tonio Buonassisi

Citation: *J. Appl. Phys.* **112**, 084508 (2012); doi: 10.1063/1.4758305

View online: <http://dx.doi.org/10.1063/1.4758305>

View Table of Contents: <http://jap.aip.org/resource/1/JAPIAU/v112/i8>

Published by the [American Institute of Physics](http://www.aip.org).

---

### Related Articles

The anomalous Hall effect in the perpendicular Ta/CoFeB/MgO thin films

*J. Appl. Phys.* **113**, 17C717 (2013)

Thermal stability of metal Ohmic contacts in indium gallium zinc oxide transistors using a graphene barrier layer

*Appl. Phys. Lett.* **102**, 113112 (2013)

Full band calculations of the intrinsic lower limit of contact resistivity

*Appl. Phys. Lett.* **102**, 111605 (2013)

A comprehensive model for the electrical nanocontact on germanium for scanning spreading resistance microscopy applications

*J. Appl. Phys.* **113**, 114310 (2013)

Peculiarities of spin polarization inversion at a thiophene/cobalt interface

*Appl. Phys. Lett.* **102**, 111604 (2013)

---

### Additional information on J. Appl. Phys.

Journal Homepage: <http://jap.aip.org/>

Journal Information: [http://jap.aip.org/about/about\\_the\\_journal](http://jap.aip.org/about/about_the_journal)

Top downloads: [http://jap.aip.org/features/most\\_downloaded](http://jap.aip.org/features/most_downloaded)

Information for Authors: <http://jap.aip.org/authors>

## ADVERTISEMENT



**AIP Advances**

Now Indexed in Thomson Reuters Databases

Explore AIP's open access journal:

- Rapid publication
- Article-level metrics
- Post-publication rating and commenting

## Low contact resistivity of metals on nitrogen-doped cuprous oxide (Cu<sub>2</sub>O) thin-films

Sin Cheng Siah,<sup>a)</sup> Yun Seog Lee, Yaron Segal, and Tonio Buonassisi<sup>b)</sup>  
*Massachusetts Institute of Technology, Cambridge, Massachusetts 02139, USA*

(Received 9 July 2012; accepted 12 September 2012; published online 19 October 2012)

Forming low-resistivity contacts on cuprous oxide (Cu<sub>2</sub>O) is an essential step toward demonstrating its suitability as a candidate solar cell material. We measure the contact resistivity of three noble metals (Au, Ag, and Pd) on sputtered Cu<sub>2</sub>O thin-films with a range of nitrogen doping levels. Using the circular transmission line model, specific contact resistivity as low as  $1.1 \times 10^{-4} \Omega \cdot \text{cm}^2$  is measured for Pd contacts on heavily doped Cu<sub>2</sub>O films. Temperature-dependent current-voltage measurements and X-ray photoemission spectroscopy are used to determine the barrier heights formed at metal/Cu<sub>2</sub>O interfaces. Thermionic emission is observed to dominate for undoped films, whilst field emission dominates for heavily doped films, highlighting the importance of carrier concentration on contact resistivity. Finally, we demonstrate that low contact resistivity can be achieved on heavily doped Cu<sub>2</sub>O films using Earth-abundant metals, such as Cu and Ni. © 2012 American Institute of Physics. [<http://dx.doi.org/10.1063/1.4758305>]

### I. INTRODUCTION

Cuprous oxide (Cu<sub>2</sub>O), a compound semiconductor with a direct bandgap of 1.9–2.1 eV,<sup>1</sup> is a promising material for thin-film photovoltaic applications due to its elemental abundance<sup>2</sup> in the Earth's crust and non-toxicity. Polycrystalline Cu<sub>2</sub>O thin-films and wafers have been grown by various techniques, including reactive DC magnetron sputtering,<sup>3</sup> electrochemical deposition,<sup>4</sup> molecular beam epitaxy,<sup>5</sup> and thermal oxidation of Cu metal foils.<sup>6</sup> To date, conversion efficiencies of Cu<sub>2</sub>O-based solar cells have been low (record efficiency 3.83%)<sup>6</sup> due to bulk non-radiative recombination,<sup>7</sup> recombination through interface defect states,<sup>6</sup> and high series resistance. A systematic investigation into each loss mechanism is needed to improve the efficiency of Cu<sub>2</sub>O-based devices.

Forming low-resistivity ohmic contacts on cuprous oxide (Cu<sub>2</sub>O) is an essential step to reduce resistive power loss and enhance device performance of Cu<sub>2</sub>O-based solar cells. A contact resistivity ( $\rho_c$ ) lower than  $2 \times 10^{-3} \Omega \cdot \text{cm}^2$  is desired for conventional Si-based solar cells.<sup>8</sup> To form ohmic contacts on Cu<sub>2</sub>O, Au has been the material of choice,<sup>6,7</sup> due to its favorably large work function and low chemical reactivity. However, no contact resistivity measurements of metals on Cu<sub>2</sub>O films have been reported.

In this work, we measure the  $\rho_c$  of metal/Cu<sub>2</sub>O interface using various metals, including Au, Ag, Pd, Cu, and Ni. We study the effect of Cu<sub>2</sub>O doping level on the contact resistivity and the carrier transport mechanism. The three noble metal candidates are selected based on their high work functions ( $\phi_{\text{Ag}} = 4.74$  eV,  $\phi_{\text{Au}} = 5.31$  eV, and  $\phi_{\text{Pd}} = 5.60$  eV)<sup>9</sup> and low reactivity with Cu<sub>2</sub>O as determined by the standard free energies of metal-oxide formation at room temperature ( $\Delta G_{298\text{K}}^{\text{Cu}_2\text{O}} = -147.2$  kJ,<sup>10</sup>  $\Delta G_{298\text{K}}^{\text{PdO}} = -82.1$  kJ,<sup>10</sup>  $\Delta G_{298\text{K}}^{\text{Ag}_2\text{O}} = -10.8$  kJ<sup>10</sup>, and  $\Delta G_{298\text{K}}^{\text{Au}_2\text{O}} > 0$ ). We show that it is

possible to obtain  $\rho_c$  as low as  $1.1 \times 10^{-4} \Omega \cdot \text{cm}^2$  on nitrogen-doped (N-doped) Cu<sub>2</sub>O films, indicating the importance of doping to achieve low  $\rho_c$ . Finally, we demonstrate that  $\rho_c < 10^{-3} \Omega \cdot \text{cm}^2$  can be achieved for Earth-abundant metals, such as Cu and Ni, by forming a tunneling junction with N-doped Cu<sub>2</sub>O.

### II. EXPERIMENTAL METHODS

The Cu<sub>2</sub>O thin-films in this study were grown using reactive direct-current magnetron sputtering on GE-124 fused quartz glass substrates. A metallic copper target (99.999% pure, K. J. Lesker) was sputtered in an argon, oxygen, and nitrogen ambient. The film's doping level was controlled by varying the flow of N<sub>2</sub> gas between 0 and 4 sccm during the sputtering process. Film electrical resistivities and hole concentrations were characterized by four-point probe and Hall effect measurements, respectively. X-ray diffraction was used to confirm that all films contained pure Cu<sub>2</sub>O phase. Film thicknesses were determined by cross-sectional scanning electron microscopy. Films' nitrogen concentrations were measured using secondary ion mass spectrometry (SIMS) with a calibration sample prepared by a controlled amount of nitrogen implantation.

The parameter  $\rho_c$  on nominally undoped and N-doped films was determined using the circular transmission line model (CTLM).<sup>11</sup> The circular transmission line patterns with inner-outer ring spacings of 4 to 12  $\mu\text{m}$  were achieved by photoresist lift-off of electron-beam-evaporated 100 nm films of Au, Ag, Pd, Cu, and Ni. The total resistance across the contact spacing can be expressed by the relation<sup>12</sup>

$$R_t = \frac{R_s}{2\pi} \left[ \ln\left(\frac{r}{r-d}\right) + L_t \left( \frac{1}{r} + \frac{1}{r-d} \right) \right], \quad (1)$$

where  $R_s$  is the sheet resistance of the Cu<sub>2</sub>O film,  $r$  is the radius of the outer circular contact pad,  $d$  is the width of the ring, and  $L_t$  is the transfer length. Least squares curve fitting

<sup>a)</sup> Author to whom correspondence should be addressed. Electronic mail: [siahsincheng@gmail.com](mailto:siahsincheng@gmail.com).

<sup>b)</sup> Electronic mail: [buonassisi@mit.edu](mailto:buonassisi@mit.edu).

was used to extract the parameters  $R_s$  and  $L_t$ ; subsequently,  $\rho_c$  can be obtained from the relation<sup>11</sup>

$$L_t = \sqrt{\rho_c/R_s}. \quad (2)$$

X-ray photoemission spectroscopy (XPS) analyses were conducted on undoped  $\text{Cu}_2\text{O}$  films with 1, 2, and 3 nm of metallic overlayers deposited using electron-beam evaporation at a rate of  $0.5 \text{ \AA/s}$ . The XPS measurements were performed using a monochromated  $\text{Al-K}\alpha$  source (photon energy  $1486.6 \text{ eV}$ ), and the films were grounded using silver-painted contacts. We monitored the adventitious C  $1s$  peak to account for any residual charging. Finally, to elucidate the electron transport mechanism across the metal/ $\text{Cu}_2\text{O}$  interface, temperature-dependent  $\rho_c$  measurements were performed on a heated chuck and I-V characteristics were recorded over the temperature range  $280\text{--}390 \text{ K}$  monitored externally through a thermocouple.

### III. RESULTS AND DISCUSSION

#### A. Undoped $\text{Cu}_2\text{O}$ /metal contacts: Schottky barrier height (SBH) and chemical reactivity

To measure the SBH and investigate the chemical reactivity at the contact between metal and undoped  $\text{Cu}_2\text{O}$ , we performed XPS analysis on undoped  $\text{Cu}_2\text{O}$  films covered with 1, 2, and 3 nm of metallic overlayers. Figure 1 shows the Cu  $2p$  core level signals for the three different metals as a function of metal film thickness. One observes two distinguishing features that set Pd apart from the other metals: (1) the measured peak intensities for the samples covered in Pd attenuate more rapidly with increasing thickness compared to Au and Ag; (2) the Cu  $2p$  core level peak energy shifts to lower values with increasing Pd thickness. We will return to these observations after a discussion of Schottky barrier heights.

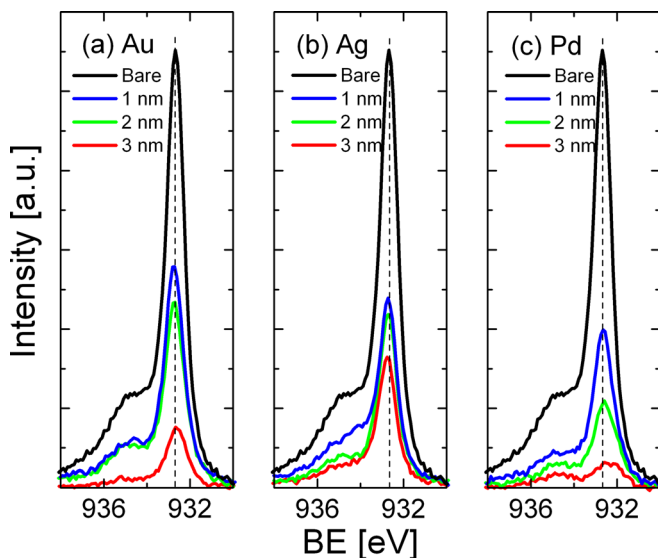


FIG. 1. Cu  $2p$  core level photoemission for (a) Au, (b) Ag, and (c) Pd samples. A peak shift towards lower binding energies is observed for the Pd samples, indicating the lowering of the SBH. A high binding energy shoulder due to  $\text{CuO}$  can be observed. All spectra have been corrected for charging by using the adventitious C  $1s$  peak.

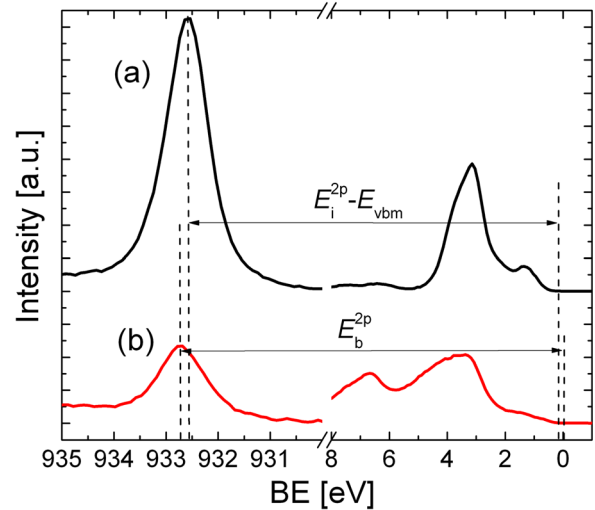


FIG. 2. Illustration of method to determine the SBH from the XPS data from the valence-band spectra (right) and Cu  $2p$  core level spectra (left) of (a) bare  $\text{Cu}_2\text{O}$  film and (b)  $\text{Cu}_2\text{O}$  film with 2 nm Au overlayer. The Fermi level is calibrated using the Fermi edge of Au. All spectra have been corrected for charging by using the adventitious C  $1s$  peak.

By analysing the band bending at the metal/ $\text{Cu}_2\text{O}$  interface as illustrated in Fig. 2, the SBH can be determined from the XPS data using the relation<sup>13</sup>

$$\phi_b = E_b^{2p} - [E_i^{2p} - E_{VBM}], \quad (3)$$

where  $E_b^{2p}$  is the binding energy of the Cu  $2p$  core level of  $\text{Cu}_2\text{O}$  film with a metal overlayer,  $E_i^{2p}$  is the binding energy of Cu  $2p$  core level for a bare  $\text{Cu}_2\text{O}$  film, and  $E_{VBM}$  is the position of the valence band maximum. All binding energies are referenced to the Fermi level of the instrument,  $E_F$ , which is calibrated using the Fermi edge of Au. SBH values obtained by analyzing the 2 nm thick overlayer signal are  $0.3 \pm 0.1 \text{ eV}$ ,  $0.4 \pm 0.1 \text{ eV}$ , and  $0.2 \pm 0.1 \text{ eV}$  for Au, Ag, and Pd, respectively. The 2 nm thick samples are compared, as the Cu  $2p$  core level signal of the Pd 3 nm sample is too low to be used for meaningful analysis.

In addition, to obtain the SBH values at metal/ $\text{Cu}_2\text{O}$  interfaces, we also fit the  $\rho_c$  vs. temperature curves (Fig. 5) for the undoped samples using the standard thermionic emission (TE) model given by<sup>8</sup>

$$\rho_c = \frac{k}{qA^*T} e^{\frac{q\phi_b}{kT}}, \quad (4)$$

where  $k$  is Boltzmann's constant,  $A^*$  is the effective Richardson's constant,  $T$  is the absolute measurement temperature, and  $\phi_b$  is the SBH. We treat  $A^*$  and  $\phi_b$  as fitting parameters. The fitted values for SBH are  $0.23 \pm 0.01 \text{ eV}$ ,  $0.17 \pm 0.01 \text{ eV}$ , and  $0.14 \pm 0.01 \text{ eV}$  for Au, Ag, and Pd, respectively.

Table I summarizes the values of SBH obtained using XPS and CTLM. Both XPS and CTLM methods measure the lowest SBH for the Pd sample. We believe this is due to more significant shifting of the Fermi level toward the valence band maximum of  $\text{Cu}_2\text{O}$  at the Pd/ $\text{Cu}_2\text{O}$  interface. This effect can be explained from Fig. 1, which shows the



TABLE I. Comparison of Schottky barrier heights obtained from XPS and CTLM.

Metal	XPS (2 nm) [eV]	CTLM (100 nm) [eV]
Au	$0.3 \pm 0.1$	$0.23 \pm 0.01$
Ag	$0.4 \pm 0.1$	$0.17 \pm 0.01$
Pd	$0.2 \pm 0.1$	$0.14 \pm 0.01$

Cu  $2p$  core level peak shifting toward lower binding energies as the thickness of the metal overlayer increases.<sup>14</sup> Insignificant peak shifts are observed for both Au and Ag. This results in the lowest effective SBH for the Pd/Cu<sub>2</sub>O structure.

An additional effect may contribute to lowering the Pd-Cu<sub>2</sub>O contact resistivity relative to Ag and Au. In XPS measurements, the core level intensity is observed to attenuate more strongly with increasing Pd overlayer thickness than either Au or Ag. From other studies,<sup>15</sup> XPS peak attenuation is known to depend on overlayer thickness, metal coverage uniformity, and photoelectron attenuation length of the overlayer material. By comparing electron inelastic mean free paths for Au (16.5 Å, 1400 eV), Ag (15.2 Å, 1100 eV), and Pd (19.6 Å, 1100 eV) as calculated by Tanuma *et al.*,<sup>16</sup> one would expect the Cu  $2p$  core level signal of the Ag and Au samples to attenuate most rapidly because of electron scattering. However, the Cu  $2p$  core level peak intensity for the Pd sample is the lowest despite having the largest electron inelastic mean free path. This may indicate that Pd wets the surface more effectively than Au and Ag.

The metal core level peaks for 2 nm overlayer thickness are shown in Fig. 3. Sharp, well-defined peaks can be observed for both Au and Ag, indicating that the Au and Ag are in a metallic chemical state. This is in agreement with the thermodynamic data mentioned earlier, as Au and Ag oxide formation energies are relatively unfavorable. A high binding energy shoulder can be observed for the Pd sample, which we attribute to PdO.<sup>17</sup> The hypothesized superior wet-

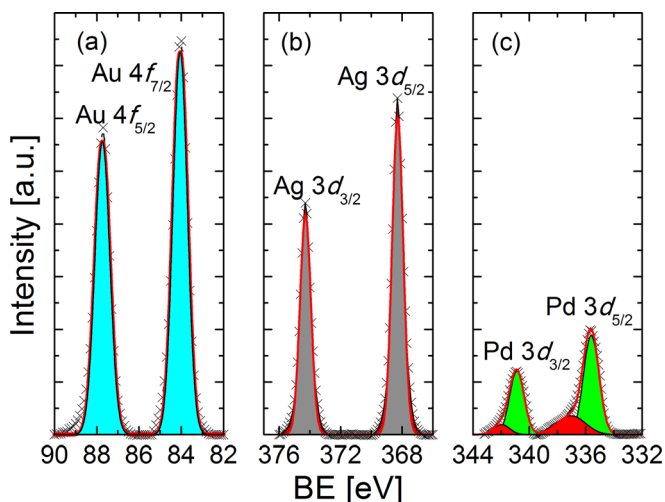


FIG. 3. Photoemission from metallic peaks of samples with 2 nm thick (a) Au, (b) Ag, and (c) Pd overlayers. A high binding energy shoulder due to PdO can be observed.

ting characteristics of Pd on Cu<sub>2</sub>O could be related to the formation of PdO. This observation is consistent with the findings of Pan *et al.*<sup>18</sup> In this case, the formation of interfacial Pd-O bonds might contribute to the reduction of the overall free energy and promote a Frank-van der Merwe (layer-by-layer) type growth for Pd.<sup>18</sup> The good coverage by the metal film mediated by interfacial PdO formation may lead to higher-quality metal/Cu<sub>2</sub>O junction and lower  $\rho_c$  for undoped Cu<sub>2</sub>O films. If this interpretation is correct, then chemical inertness may not be the most important parameter defining an ideal contact metal for undoped Cu<sub>2</sub>O.

## B. Nitrogen doping reduces metal/Cu<sub>2</sub>O contact resistivity and changes the conduction mechanism

Introducing nitrogen gas during Cu<sub>2</sub>O film growth is observed to reduce film electrical resistivity at room temperature.<sup>19</sup> An undoped Cu<sub>2</sub>O film exhibits a resistivity of 56  $\Omega \cdot \text{cm}$ , while N-doped films have resistivities of 4.4 and 0.4  $\Omega \cdot \text{cm}$  for nitrogen concentrations ([N]) 0.6 and 1.2 atomic (at.%) , respectively. From Hall effect measurements, hole concentrations of undoped and N-doped ([N]=0.6 at.%) films are measured to be  $3.7 \times 10^{15} \text{ cm}^{-3}$  and  $1.8 \times 10^{18} \text{ cm}^{-3}$ , respectively. Due to a low Hall mobility, we are unable to accurately measure the hole concentration of the heavily doped film ([N] = 1.2 at. %).

Figure 4 shows a plot of  $\rho_c$  for the three inert contact metals (Au, Ag, and Pd) and different nitrogen doping densities. It is observed that Pd exhibits the lowest  $\rho_c$  on undoped Cu<sub>2</sub>O films, while  $\rho_c$  as low as  $1.1 \times 10^{-4} \Omega \cdot \text{cm}^2$  is obtained on highly doped Cu<sub>2</sub>O. While  $\rho_c$  can vary over an order of magnitude on undoped films for the three different metals, less variation is observed for doped films.

To gain insight into the conduction mechanism, in Fig. 5 we compare the temperature dependence of  $\rho_c$  of Pd for three different Cu<sub>2</sub>O nitrogen doping concentrations. For the highly doped sample,  $\rho_c$  shows a weak dependence on the measurement temperature, whereas  $\rho_c$  of the undoped sample exhibits an Arrhenius-type dependence on temperature. Similar behavior is observed for Au and Ag samples. This

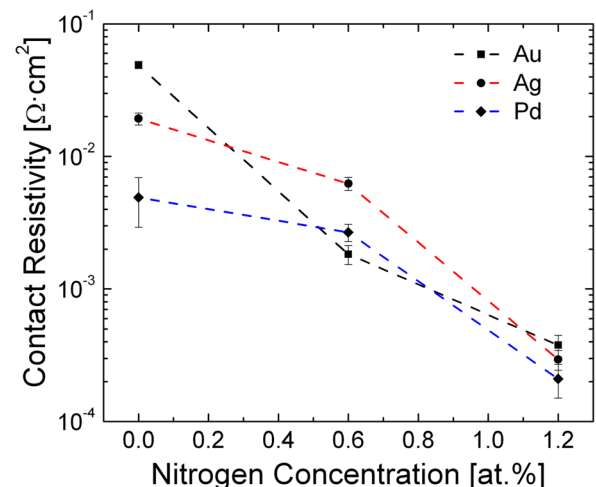


FIG. 4. Contact resistivity is plotted against Cu<sub>2</sub>O nitrogen doping concentration for three contact metals: Au, Ag, and Pd.

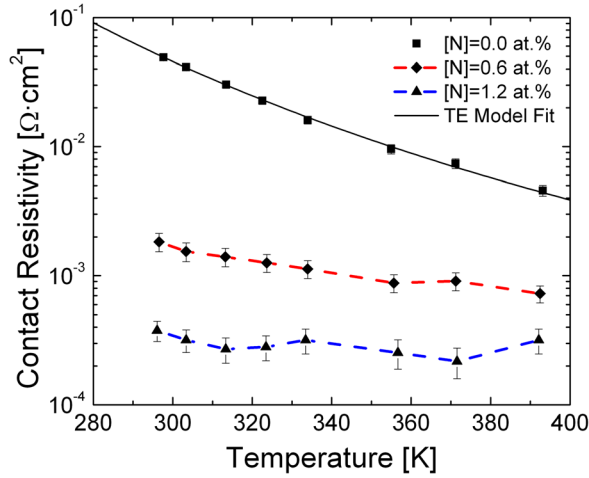


FIG. 5. Contact resistivity as a function of measurement temperature for Pd on Cu<sub>2</sub>O with three doping concentrations. Similar behavior (not shown) is also observed for Au and Ag samples. The solid black line represents a fit to a thermionic emission model; the dashed red and blue lines are guides to the eye.

indicates that at low doping densities, the dominating conduction mechanism is TE. In this regime,  $\rho_c$  decreases as temperature increases and a greater number of electrons possess sufficient thermal energy to overcome the Schottky barrier at the metal/Cu<sub>2</sub>O interface.<sup>8</sup> As doping densities increase, the Schottky barrier becomes sufficiently narrow and carrier transport becomes increasingly dominated by field emission (FE), which is only weakly temperature dependent. To support these observations, we plot the ratio  $kT/E_{00}$  as a function of hole densities ( $p$ ) (Fig. 6). The parameter  $E_{00}$  is related to the tunneling probability and is defined as<sup>20</sup>

$$E_{00} = \frac{q\hbar}{2} \sqrt{\frac{p}{m^*\epsilon}}, \quad (5)$$

where  $\hbar$  is the reduced Planck's constant,  $q$  is electronic charge,  $m^*$  is taken to be  $0.58m_0$  (Ref. 21) where  $m_0$  is the

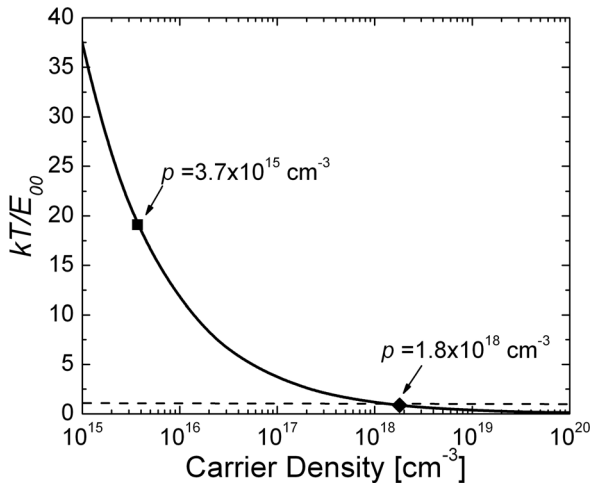


FIG. 6. Plot of the ratio  $kT/E_{00}$  as a function of hole density ( $p$ ) with  $m^* = 0.58m_0$  and  $\epsilon = 7\epsilon_0$ . The dashed line indicates that the ratio  $kT/E_{00} = 1$  and both thermionic emission and field effect processes are comparable.  $kT/E_{00}$  for both undoped ( $[N] = 0.0$  at. %,  $p = 3.7 \times 10^{15} \text{ cm}^{-3}$ ) and lightly ( $[N] = 0.6$  at. %,  $p = 1.8 \times 10^{18} \text{ cm}^{-3}$ ) doped samples are indicated on the plot.

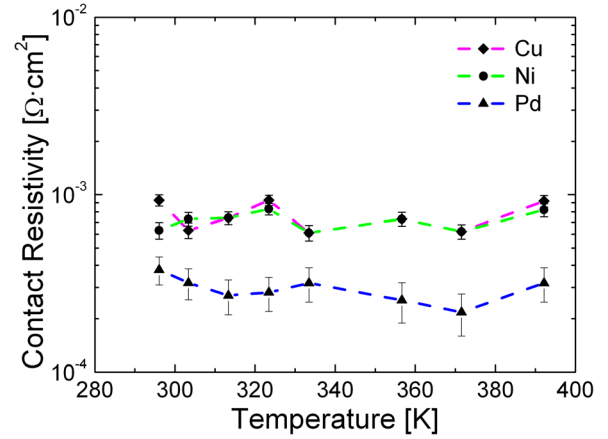


FIG. 7. Contact resistivity as a function of measurement temperature for Cu, Ni, and Pd on highly doped ( $[N] = 1.2$  at. %) samples. The dashed lines are guides to the eye.

free electron mass, and  $\epsilon$  is the dielectric constant of Cu<sub>2</sub>O taken to be  $7\epsilon_0$ .<sup>21</sup> In this case, the ratio  $kT/E_{00}$  is a measure of the relative contribution of the TE to tunneling process.<sup>20</sup> It can be observed from Fig. 6 that for lightly doped Cu<sub>2</sub>O ( $p < 10^{18} \text{ cm}^{-3}$ ),  $kT/E_{00} \gg 1$  and thus, TE is dominant. At intermediate doping levels ( $p \approx 10^{18} \text{ cm}^{-3}$ ),  $kT/E_{00} \approx 1$  and the carrier transport is in the thermionic field emission regime where both thermionic and tunneling processes are comparable. Finally, at very high doping levels ( $p > 10^{19} \text{ cm}^{-3}$ ),  $kT/E_{00} \ll 1$  and carrier transport is dominated by FE where current is carried by holes tunneling across the junction. As such, the calculated functional dependence of  $kT/E_{00}$  with  $p$  is in good agreement with the observations made based on the temperature dependence of  $\rho_c$ .

### C. Nitrogen doping enables low-resistivity contact for Earth-abundant metals

We demonstrate that it is possible to form low resistivity ohmic contacts to N-doped Cu<sub>2</sub>O using Cu and Ni, both Earth-abundant metals. We achieve  $\rho_c$  of  $9.3 \times 10^{-4}$  and  $6.3 \times 10^{-4} \Omega \cdot \text{cm}^2$  for Cu and Ni contacts, respectively, on Cu<sub>2</sub>O doped with  $[N] = 1.2$  at. %. Temperature-dependent TLM measurements (Fig. 7) indicate that  $\rho_c$  for both Cu and Ni on N-doped Cu<sub>2</sub>O films have weak temperature dependence. This suggests that FE is the dominating carrier transport mechanism across the metal/Cu<sub>2</sub>O interface, consistent with observations involving noble metals.

### IV. CONCLUSIONS

We examine the doping-level dependence of contact resistance for three noble metals on Cu<sub>2</sub>O films: Pd, Ag, and Au. For all metals, we observe an inverse dependence of contact resistivity on Cu<sub>2</sub>O nitrogen doping concentration. At low carrier densities, a TE model describes the interface charge transport mechanism. At high Cu<sub>2</sub>O carrier densities, a FE model accurately describes conduction across the metal/Cu<sub>2</sub>O interface, indicating the formation of a tunneling junction with  $kT/E_{00} < 1$ . In such samples,  $\rho_c$  as low as  $1.1 \times 10^{-4} \Omega \cdot \text{cm}^2$  is achieved. Using this approach, we

showed that it is possible to obtain  $\rho_c < 10^{-3} \Omega \cdot \text{cm}^2$  on N-doped  $\text{Cu}_2\text{O}$  films using Earth-abundant metals, such as Cu and Ni.

An interesting observation is that Pd is the best candidate for forming low-resistivity ohmic contacts on undoped  $\text{Cu}_2\text{O}$  due to the low effective Schottky barrier height at the metal/ $\text{Cu}_2\text{O}$  interface. XPS measurements suggest that the good electrical contact of Pd on undoped  $\text{Cu}_2\text{O}$  may be due to the formation of an interfacial PdO layer that aids in the wetting of the  $\text{Cu}_2\text{O}$  surface, and bending of the  $\text{Cu}_2\text{O}$  valence band maximum toward the metal Fermi energy at the Pd/ $\text{Cu}_2\text{O}$  interface as observed from the shift in the Cu  $2p$  core levels. Further work may elucidate the degree to which the best candidate contact metals on lowly doped substrates may be predicted not solely on the basis of work function, but on the basis of a complex interrelationship between chemical inertness, wettability, stress, chemical potential, and semiconductor free carrier density, among other parameters.

## ACKNOWLEDGMENTS

The authors thank S. Speakman and E. Macomber for equipment support, M. T. Winkler for performing Hall measurements, and H. A. Atwater for an inspirational discussion regarding Earth-abundant metal contacts. This work was supported by Chesonis Family Foundation and an MIT Energy Initiative seed grant and by Bosch through the MIT Energy Initiative. This work made use of the MRSEC Shared Experimental Facilities at MIT and the Center for Nanoscale Systems at Harvard University supported by NSF awards DMR-0819762 and ECS-0335765, respec-

tively. A Clean Energy Scholarship from NRF Singapore (S.C.S) and an NSF CAREER award ECCS-1150878 (T.B.) are acknowledged.

- <sup>1</sup>F. L. Weichman, *Phys. Rev.* **117**, 998 (1960).
- <sup>2</sup>C. Wadia, A. P. Alivisatos, and D. M. Kammen, *Environ. Sci. Technol.* **43**, 2072 (2009).
- <sup>3</sup>Y. S. Lee, M. T. Winkler, S. C. Siah, R. Brandt, and T. Buonassisi, *Appl. Phys. Lett.* **98**, 192115 (2011).
- <sup>4</sup>Y. Luo, L. Wang, Y. Zuo, X. Sheng, L. Chang, and D. Yang, *Electrochem. Solid-State Lett.* **15**, H34 (2012).
- <sup>5</sup>D. S. Darvish and H. A. Atwater, *J. Cryst. Growth* **319**, 39 (2011).
- <sup>6</sup>T. Minami, Y. Nishi, T. Miyata, and J. Nomoto, *Appl. Phys. Express* **4**, 062301 (2011).
- <sup>7</sup>S. O. Ishizuka, K. Suzuki, Y. Okamoto, M. Yanagita, T. Sakurai, and K. Akimoto, *Phys. Status Solidi C* **1**, 1067 (2004).
- <sup>8</sup>D. K. Schroder, *IEEE Trans. Electron. Devices* **31**, 637 (1984).
- <sup>9</sup>W. M. Haynes and D. R. Lide, *CRC Handbook of Chemistry and Physics*, 91st ed. (CRC Press, Cleveland, 2011).
- <sup>10</sup>E. T. Turkdogan, *Physical Chemistry of High Temperature Technology* (Academic, New York, 1980).
- <sup>11</sup>G. K. Reeves, *Solid State Electron.* **23**, 487 (1980).
- <sup>12</sup>H. S. Yang, Y. Li, D. P. Norton, K. Ip, S. J. Pearton, S. Jang, and F. Ren, *Appl. Phys. Lett.* **86**, 192103 (2005).
- <sup>13</sup>Y. Y. Mi, S. J. Wang, Y. F. Dong, J. W. Chai, J. S. Pan, A. C. H. Huan, and C. K. Ong, *Surf. Sci.* **599**, 255 (2005).
- <sup>14</sup>J. S. Jang and T. Y. Seong, *J. Appl. Phys.* **88**, 3064 (2000).
- <sup>15</sup>K. A. Rickert, A. B. Ellis, J. K. Kim, J. L. Lee, F. J. Himpsel, F. Dwikusuma, and T. F. Kuech, *J. Appl. Phys.* **92**, 6671 (2002).
- <sup>16</sup>S. Tanuma, C. J. Powell, and D. R. Penn, *Surf. Interface Anal.* **17**, 927 (1991).
- <sup>17</sup>M. Brun, A. Berthet, and J. C. Bertolini, *J. Electron Spectrosc.* **104**, 55 (1999).
- <sup>18</sup>J. Pan, U. Diebold, L. Zhang, and T. Madey, *Surf. Sci.* **295**, 411 (1993).
- <sup>19</sup>S. I. Shizuka, S. K. Ato, T. M. Aruyama, and K. A. Kimoto, *Jpn. J. Appl. Phys.* **40**, 2765 (2001).
- <sup>20</sup>A. Y. C. Yu, *Solid State Electron.* **13**, 239 (1970).
- <sup>21</sup>F. Biccari, C. Malerba, and A. Mittiga, *Sol. Energy Mater. Sol. Cells* **94**, 1947 (2010).